Turbulent dynamo in a collisionless plasma

François Rincon[a,b,1], Francesco Califano[c], Alexander A. Schekochihin[d,e], and Francesco Valentini[f]

[a]Université de Toulouse, Université Paul Sabatier-Observatoire Midi-Pyrénées, Institut de Recherche en Astrophysique et Planétologie, F-31400 Toulouse, France; [b]CNRS, Institut de Recherche en Astrophysique et Planétologie, F-31400 Toulouse, France; [c]Physics Department, University of Pisa, 56127 Pisa, Italy; [d]The Rudolf Peierls Centre for Theoretical Physics, University of Oxford, Oxford OX1 3NP, United Kingdom; [e]Merton College, Oxford OX1 4JD, United Kingdom; and [f]Dipartimento di Fisica, Universitá della Calabria, I-87036 Rende (CS), Italy

Edited by Neta A. Bahcall, Princeton University, Princeton, NJ, and approved March 1, 2016 (received for review December 21, 2015)

Magnetic fields pervade the entire universe and affect the formation and evolution of astrophysical systems from cosmological to planetary scales. The generation and dynamical amplification of extragalactic magnetic fields through cosmic times (up to microgauss levels reported in nearby galaxy clusters, near equipartition with kinetic energy of plasma motions, and on scales of at least tens of kiloparsecs) are major puzzles largely unconstrained by observations. A dynamo effect converting kinetic flow energy into magnetic energy is often invoked in that context; however, extragalactic plasmas are weakly collisional (as opposed to magnetohydrodynamic fluids), and whether magnetic field growth and sustainment through an efficient turbulent dynamo instability are possible in such plasmas is not established. Fully kinetic numerical simulations of the Vlasov equation in a 6D-phase space necessary to answer this question have, until recently, remained beyond computational capabilities. Here, we show by means of such simulations that magnetic field amplification by dynamo instability does occur in a stochastically driven, nonrelativistic subsonic flow of initially unmagnetized collisionless plasma. We also find that the dynamo self-accelerates and becomes entangled with kinetic instabilities as magnetization increases. The results suggest that such a plasma dynamo may be realizable in laboratory experiments, support the idea that intracluster medium turbulence may have significantly contributed to the amplification of cluster magnetic fields up to near-equipartition levels on a timescale shorter than the Hubble time, and emphasize the crucial role of multiscale kinetic physics in high-energy astrophysical plasmas.

magnetic fields | dynamo | turbulence | intracluster medium

The generation, amplification, and sustainment of magnetic fields in nature may be driven by a variety of physical processes, an important family of which is dynamo instabilities converting kinetic energy of chaotic flows into magnetic energy. Although fluid (collisional) magnetohydrodynamic (MHD) dynamos relevant to the planetary, stellar, and galactic contexts had long been thought possible on the basis of idealized theoretical models of turbulent flows (1–4), a major boost to their understanding was given by early pioneering numerical simulations of magnetic field amplification by 3D MHD turbulence (5), a rare case of proof of principle "numerical discovery" later followed by experimental evidence using liquid metals (6). Dynamos in weakly collisional plasmas, despite their potential relevance to cosmic magnetogenesis (7, 8) on extragalactic scales (9–18), have, thus far, not achieved such a milestone. Although dedicated laboratory experiments are under development (19, 20), the interactions between dynamos, collisionless damping, and kinetic-scale phenomena related to plasma magnetization are poorly understood. Magnetization occurs when the field has grown sufficiently that the particles' Larmor radius becomes smaller than the typical size ℓ of velocity fluctuations. It does not take much field to achieve this: in the intracluster medium, taking $\ell = 1$ kiloparsec and $\sim 10^7$ K ion temperature, ions are magnetized for fields above 10^{-13} G, well below the level at which magnetic energy reaches equipartition with kinetic energy of plasma motions. Past this stage, any local change in magnetic field strength caused by compressive or shearing motions will generate pressure anisotropies with respect to the field by virtue of magnetic moment conservation, rendering the plasma everywhere unstable to fast kinetic instabilities (12), with potentially critical implications for magnetic growth and dynamics (16, 17, 21–27). Showing whether collisionless plasma dynamos exist and how they work requires solving Vlasov–Maxwell equations in three physical space dimensions [3D; this stems from antidynamo theorems in 2D (4)] plus three velocity space dimensions (3V). We performed the first, to our knowledge, numerical simulations of this problem, which show that magnetic field amplification through a turbulent collisionless plasma dynamo occurs in both unmagnetized and magnetized regimes.

Problem Formulation

Our model (*Material and Methods*) describes the coupled evolution of a quasineutral, nonrelativistic plasma of collisionless protons (mass m_i), isothermal fluid electrons of negligible inertia, and electromagnetic fields **E** and **B**. It formally retains magnetic advection and induction, resistivity, and the Hall effect but because of the isothermal electrons assumption, does not allow for a Biermann battery (28) or Weibel-like instabilities (13, 29) (these effects only generate very small seed fields and are not themselves viable dynamos). The equations are solved with a 3D–3V Eulerian numerical code in a periodic cubic spatial domain of size $L = 2{,}000\,\pi\, d_i$, where d_i is the ion inertial length, and a velocity space range of ± 5 ion thermal speeds $v_{\mathrm{th}i}$. The system is initialized with a Maxwellian ion distribution function of uniform density n_{i0}, temperature $T_i = m_i v_{\mathrm{th}i}^2/2$, electron temperature $T_e = T_i$, and a magnetic seed in the wavenumber range $[2\pi/L, 4\pi/L]$. The field strength, characterized by the inverse of $\beta = 8\pi\, n_{i0} T_i / B_{\mathrm{rms}}^2$, remains small enough ($\beta \gg 1$) that the Hall effect is negligible,

ASTRONOMY

Significance

Although magnetic field amplification by a dynamo effect converting kinetic flow energy into magnetic energy has long been shown in conventional magnetohydrodynamic fluids, whether a similar effect is possible in more dynamically complex weakly collisional plasmas, such as those encountered in astrophysical objects on extragalactic scales, is not known. We present the first, to our knowledge, conclusive numerical evidence and dynamical picture of magnetic field amplification by chaotic motions in a collisionless plasma. The results suggest that such a plasma dynamo may be a realizable physical effect in "laboratory astrophysics" experiments and support the idea that turbulent dynamos may significantly contribute to the magnetization of weakly collisional high-energy density astrophysical plasmas, such as the intracluster medium of galaxy clusters.

Author contributions: F.R., F.C., A.A.S., and F.V. designed research; F.R., F.C., and A.A.S. performed research; F.R., F.C., A.A.S., and F.V. contributed new reagents/analytic tools; F.R., F.C., A.A.S., and F.V. analyzed data; and F.R. and A.A.S. wrote the paper.

The authors declare no conflict of interest.

This article is a PNAS Direct Submission.

[1]To whom correspondence should be addressed. Email: francois.rincon@irap.omp.eu.

This article contains supporting information online at www.pnas.org/lookup/suppl/doi:10.1073/pnas.1525194113/-/DCSupplemental.

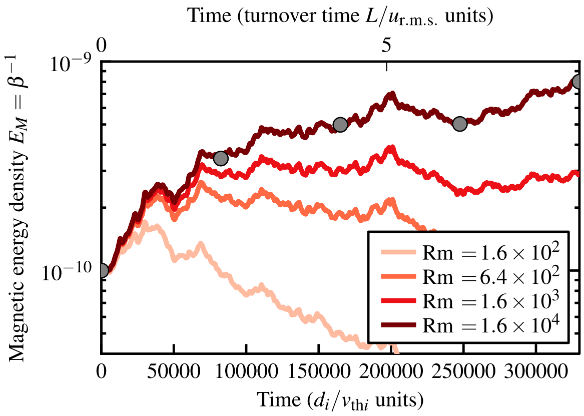

Fig. 1. Adimensionalized magnetic energy density $E_M = \beta^{-1}$ in forced simulations with decreasing magnetic diffusivities. The flow history is identical for all simulations. $L = 2{,}000\ \pi\ d_i$, $k_f = 2\pi/L$, $\varepsilon = 3 \times 10^{-5}\ n_{i0} m_i v_{\mathrm{th}i}^3/d_i$, $u_{\mathrm{rms}}/v_{\mathrm{th}i} \simeq 0.17$, and $\beta(t = 0) = 10^{10}$.

but the plasma can self-magnetize if the ion Larmor radius $\rho_i = \sqrt{\beta}\ d_i$ becomes smaller than L. An incompressible, nonhelical, stochastic external force drives a plasma flow by injecting ion momentum at system scale ($k_f = 2\pi/L$) with a prescribed average power density $\varepsilon = 3 \times 10^{-5}\ n_{i0} m_i v_{\mathrm{th}i}^3/d_i$. In unmagnetized regimes, the plasma is effectively very viscous because of the phase mixing of momentum by streaming ions (Landau damping), and therefore, the driving generates a smooth (forcing-scale) chaotic, subsonic, finite amplitude flow with a correlation time $(k_f v_{\mathrm{th}i})^{-1}$, smaller by a factor of Mach number than the turnover time $(k_f u_{\mathrm{rms}})^{-1}$, where u_{rms} is the characteristic mean ion flow velocity. This regime differs from fluid dynamo simulations, in which these timescales are comparable, and fast, inertial eddies develop down to viscous scales. The spatial and velocity space numerical resolution $64^3 \times 51^3$ is close to the current affordable maximum, because characterizing the dynamo requires several simulations, which must be integrated for several turnover times with small timesteps to capture fast kinetic physics.

Unmagnetized Regime

Fig. 1 shows the evolution of magnetic energy in four unmagnetized simulations (initial $\beta = 10^{10}$, $\rho_i/L \simeq 16$, $u_{\mathrm{rms}}/v_{\mathrm{th}i} \simeq 0.17$) with magnetic diffusivities $\eta \in [0.01, 1] v_{\mathrm{th}i}\ d_i$ [magnetic Reynolds numbers $\mathrm{Rm} = u_{\mathrm{rms}}/(k_f \eta) \in [160, 16{,}000]$] and all other parameters fixed. The results are a conclusive demonstration of plasma dynamo, with sustained magnetic growth only occurring above a critical $\mathrm{Rm} \simeq 1{,}600$ at this value of β. The magnetic energy growth rate is $\gamma \simeq 0.16(u_{\mathrm{rms}}/L)$ for the largest Rm considered. Fig. 2 (Movie S1) shows 2D snapshots of magnetic field strength and the corresponding energy spectra for the growing case. The field is stretched chaotically by velocity fluctuations and develops a characteristic folded structure with reversals perpendicular to the field at the resistive scale ℓ_η (30). The trend of the spectral evolution is consistent with the formation of a $k^{3/2}$ Kazantsev energy spectrum (1) down to $k \sim \ell_\eta^{-1}$. These results are reminiscent of a large-magnetic Prandtl number "stretch and fold" MHD dynamo (3, 4) ($\mathrm{Pm} = \nu/\eta$, where ν is the kinematic viscosity). Considering that the collisionless plasma flow is effectively very viscous, it is perhaps not a surprise that its dynamo action is similar to that of a random "Stokes flow" (30). However, the critical Rm is significantly larger than in MHD. We attribute this effect to the shorter correlation time of collisionless eddies, which limits their capacity to stretch the field in a sustained fashion.

Magnetized Regime

As the dynamo showed above proceeds, it will take the plasma from an unmagnetized to a magnetized regime. Covering the full transition is currently computationally prohibitive, because it requires integrating the 3D–3V kinetic system over many (system-scale) fluid turnover times. We, instead, investigated how magnetization affects magnetic growth using several shorter simulations initialized with seed fields of identical spatial form but different strengths ($\beta \in [10^4, 10^{10}]$) and using the same power input and $\eta = 0.1\ v_{\mathrm{th}i}\ d_i$ as in the marginally stable $\mathrm{Rm} \simeq 1{,}600$ and $\beta = 10^{10}$ case. Fig. 3 shows that the magnetic energy growth rate increases markedly with decreasing β, leading to the conclusion that magnetic growth is self-accelerating and by implication, that the critical Rm is lower at lower β (stronger seed field). We observe a transition between a "fluid-like" inductive regime and a mixed fluid–kinetic growth regime. Fig. 4 (Movie S2) shows that ion pressure anisotropies $\Delta_i = (P_{\perp,i} - P_{\parallel,i})/P_{\perp,i}$ develop with respect to the local field in the most magnetized $\beta = 10^4$ ($\rho_i/L = 0.016$) case [$\mathbf{P}_i$ is the ion pressure tensor, $P_{\parallel,i} = \hat{\mathbf{b}}\hat{\mathbf{b}} : \mathbf{P}_i$, $P_{\perp,i} = 1/2(\mathrm{Tr}\ \mathbf{P}_i - P_{\parallel,i})$, and $\hat{\mathbf{b}} = \mathbf{B}/|B|$]. Magnetic field lines develop an angular shape in strong field curvature regions of negative Δ_i, a nonlinear signature of the firehose instability, whereas bubbly mirror-like fluctuations are excited in regions of positive Δ_i, where the field is stretched (small-scale magnetic depressions are associated with overdensities) (Fig. 4, *Inset*). Relaxation of Δ_i is observed at later times in both regions. These results are consistent with theoretical expectations (12, 21, 23, 24, 27) and a scenario in which magnetization and kinetic-scale fluctuations, by impeding the free streaming of ions, enhancing particle scattering, and regulating pressure anisotropy, result in more vigorous turbulent field amplification through an effective reduction of flow viscosity (17). Higher-resolution simulations with

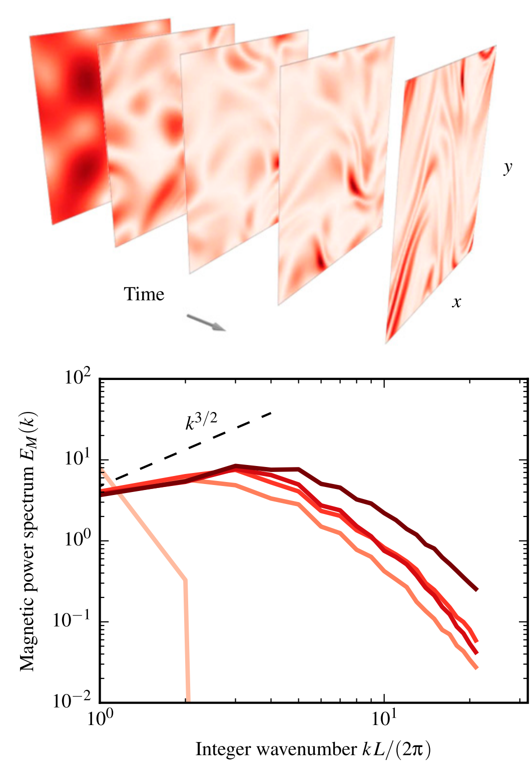

Fig. 2. (*Upper*) Cross-sections of $|B|$ at increasing times (gray circles in Fig. 1) in the $\mathrm{Rm} \simeq 16{,}000$ simulation (darker regions correspond to stronger fields; the colormap is clipped to the amplitude range of each snapshot to highlight magnetic structures). (*Lower*) Corresponding magnetic spectra (darker lines encode increasing times).

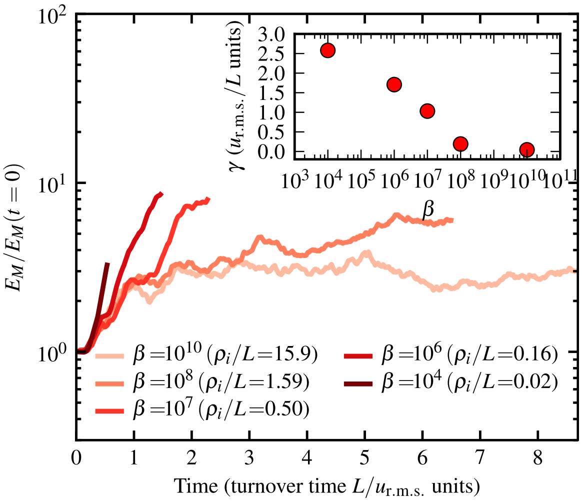

Fig. 3. Evolution of (normalized) magnetic energy density in simulations with increasing initial magnetization (decreasing β). (*Inset*) Magnetic energy growth rate vs. β. $L = 2{,}000\ \pi d_i$, $k_f = 2\pi/L$, $\varepsilon = 3\times 10^{-5}\ n_{i0} m_i v_{\mathrm{th}i}^3/d_i$, and $\eta = 0.1\ d_i\ v_{\mathrm{th}i}$.

longer integration times than can be afforded currently are required to investigate growth in this regime quantitatively.

Discussion

This paper offers a conclusive proof of principle demonstration that turbulent collisionless plasma dynamo is possible. This effect involves generic plasma processes independent of any particular geometric configuration and may, thus, be realizable in "laboratory astrophysics" plasma experiments, provided that they can achieve sufficiently weak collisionality. Numerical evidence that the dynamo becomes entangled with kinetic-scale dynamical phenomena as the plasma self-magnetizes strongly suggests that future models of weakly collisional, magnetized turbulence in high-energy astrophysical plasmas should, at least, include an effective treatment of such multiscale interactions. For now and while reconstructing the detailed history of cosmological magnetic fields remains out of reach observationally and computationally, our results provide a firmer physical basis for the idea that extragalactic plasma turbulence may significantly contribute to the amplification of seed cosmological fields up to dynamical levels on cosmologically short times, despite such plasmas not being simple collisional MHD fluids. The typical magnetic field amplification timescale in the unmagnetized regime is an appreciable fraction of the eddy turnover time, and our results suggest that the dynamo self-accelerates as magnetization takes place. In the turbulent intracluster medium, where the turnover time is believed to be no longer than 10^7 y and probably, is much shorter (17), such a dynamo could, therefore, in principle bring magnetic fields from typical $10^{-21} - 10^{-9}$ G (at most) seed field magnitudes (7, 8, 13, 14) to microgauss dynamical levels in less than a Hubble time.

New supercomputing and experimental facilities should soon make it possible to determine the parameter dependence and saturation properties of this turbulent dynamo and further assess its relevance to the coevolutions of cosmic magnetic fields and large-scale accreting structures, which are also set to be thoroughly investigated by next generation X-ray and radio observatories.

Materials and Methods

Hybrid Kinetic System. We consider a forced, nonrelativistic, quasineutral hybrid Vlasov–Maxwell system describing the coupled evolution of collisionless protons (mass m_i and charge e), fluid, isothermal electrons of temperature T_e and negligible inertia, and electromagnetic fields $\mathbf{E}(\mathbf{r},t)$ and $\mathbf{B}(\mathbf{r},t)$ ($\mathbf{r}$ and $\mathbf{v}$ are the spatial and velocity space coordinates, respectively). The ion distribution function $f_i(\mathbf{r},\mathbf{v},t)$ is governed by the Vlasov equation:

$$\frac{\partial f_i}{\partial t} + \mathbf{v}\cdot\nabla f_i + \left[\frac{e}{m_i}\left(\mathbf{E} + \frac{\mathbf{v}\times\mathbf{B}}{c}\right) + \frac{\mathbf{F}}{m_i}\right]\cdot\frac{\partial f_i}{\partial \mathbf{v}} = 0,$$

where $\mathbf{F}(\mathbf{r},t)$ is an external force described below. The ion number density is $n_i(\mathbf{r},t) = \int f_i(\mathbf{r},\mathbf{v},t)\ d^3\mathbf{v}$, the mean "fluid" ion velocity is $\mathbf{u}_i(\mathbf{r},t) = \int \mathbf{v} f_i(\mathbf{r},\mathbf{v},t) d^3\mathbf{v}/n_i$, and the ion pressure tensor is $\mathbf{P}_i(\mathbf{r},t) = m_i \int (\mathbf{v}-\mathbf{u}_i)(\mathbf{v}-\mathbf{u}_i) f_i(\mathbf{r},\mathbf{v},t) d^3\mathbf{v}$. The electron number density n_e is equal to n_i at all times by quasineutrality. The magnetic field evolution is governed by Faraday's equation,

$$\frac{\partial \mathbf{B}}{\partial t} = -c\ \nabla\times\mathbf{E},$$

and $\nabla\cdot\mathbf{B} = 0$. The electric field is calculated from Ohm's law,

$$\mathbf{E} = -\frac{T_e \nabla n_e}{e n_e} - \frac{\mathbf{u}_e\times\mathbf{B}}{c} + \frac{4\pi\eta}{c^2}\mathbf{j},$$

where $\mathbf{j} = (c/4\pi)\ \nabla\times\mathbf{B}$ is the current density, $\mathbf{u}_e = \mathbf{u}_i - \mathbf{j}/(e n_e)$ is the mean electron velocity, and η is a uniform magnetic diffusivity. The equations are adimensionalized using the initially uniform ion density n_{i0} as a reference density, the ion inertial length $d_i = c/\omega_{pi}$ as a length scale ($\omega_{pi}^2 = 4\pi\ n_{i0}\ e^2/m_i$), and $d_i/v_{\mathrm{th}i}$ as a timescale. $\mathbf{B}$ is expressed in units of $v_{\mathrm{th}i}\sqrt{4\pi\ n_{i0}\ m_i}$, and $\mathbf{E}$ is in units of $v_{\mathrm{th}i}^2\sqrt{4\pi\ n_{i0}\ m_i}/c$. The adimensional magnetic energy density is the inverse of the plasma-β.

Numerics. The problem is solved numerically with a 3D–3V Eulerian Vlasov code (31) parallelized on 1,024 cores. The resistive term in Ohm's law is only included in Faraday's equation to ensure that dynamo modes are numerically resolved.

Stochastic Ion Momentum Forcing. An incompressible, nonhelical, Δ-correlated in time vector force $\mathbf{F}(\mathbf{r},t)$ injecting ion momentum with a prescribed statistical power density-ε is included in the numerical formulation of the ion Vlasov equation using a numerical technique borrowed from hydrodynamics (32). Defining the correlation tensor of the spatial Fourier transform of the force as

$$\langle F_{\mathbf{k},i}(t) F^*_{\mathbf{k},j}(t')\rangle = \chi(k)\delta(t-t')\left(\delta_{ij} - k_i k_j/k^2\right),$$

where brackets denote ensemble averaging, it can be shown analytically that the (linear) response to this forcing in unmagnetized, collisionless regimes is a time-dependent flow $\mathbf{u}(\mathbf{r},t)$, with correlation tensor that is

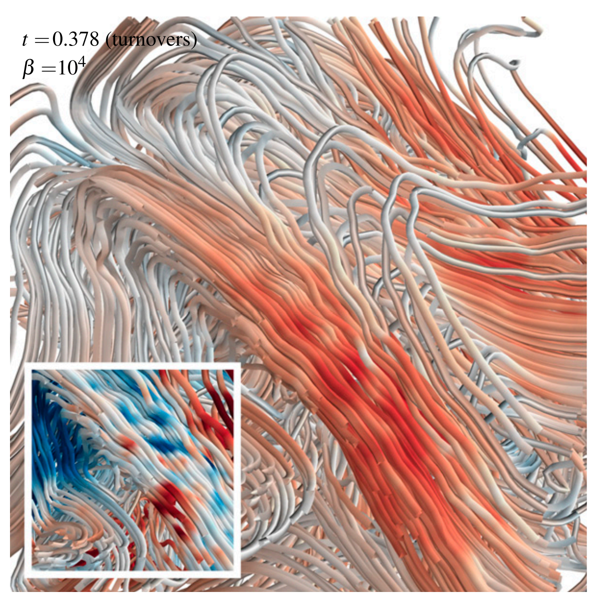

Fig. 4. 3D rendering of magnetic field lines subject to mirror and firehose instabilities in the $\beta = 10^4$ ($\rho_i/L = 0.016$) simulation (the red and blue color scale encodes positive and negative ion pressure anisotropy-Δ_i clipped to ± 1, respectively). (*Inset*) Close-up view on field lines and scalar density fluctuations in the central, mirror-unstable region [the red and blue color scale encodes $(n_i - n_{i0})/n_{i0}$ clipped to ± 1].

$$\langle u_{\mathbf{k},i}(t)u^*_{\mathbf{k},j}(t')\rangle = \frac{\chi(k)}{8\pi k^2}\left(\delta_{ij}-\frac{k_ik_j}{k^2}\right)\int_{-\infty}^{\infty} d\omega\ e^{-i\omega(t-t')}\left|Z\left(\frac{\omega}{kv_{\mathrm{th}i}}\right)\right|^2,$$

where $Z(\zeta)$ is the plasma dispersion function (33). For the forcing parameters considered here, we checked that the correlation tensor of the actual subsonic, chaotic flow driven at $k=k_f$ in unmagnetized simulations is of this form to a very good approximation, with an effective correlation time $(k_f v_{\mathrm{th}i})^{-1}$.

ACKNOWLEDGMENTS. We thank S. C. Cowley and M. W. Kunz for many valuable discussions and suggestions and C. Cavazzoni (Consorzio interuniversitario per la gestione del centro di calcolo elettronico dell' italia nord-orientale, CINECA, Italy) for his essential contribution to the code parallelization and performance. This work was granted access to the HPC resources of the Institut du développement et des ressources en informatique scientifique (IDRIS) under Allocation 2015-i2015047188 made by GENCI, and to the HPC resources of CINECA under ISCRA-B Allocation COLDYN.

1. Kazantsev AP (1968) Enhancement of a magnetic field by a conducting fluid. *Sov Phys JETP* 26:1031–1034.
2. Moffatt HK (1977) Magnetic field generation. *Electrically Conducting Fluids* (Cambridge Univ Press, Cambridge, United Kingdom).
3. Zel'dovich YB, Ruzmaikin AA, Molchanov SA, Sokoloff DA (1984) Kinematic dynamo problem in a linear velocity field. *J Fluid Mech* 144:1–11.
4. Childress S, Gilbert AD (1995) *Stretch, Twist, Fold: The Fast Dynamo* (Springer, Berlin).
5. Meneguzzi M, Frisch U, Pouquet A (1981) Helical and nonhelical turbulent dynamos. *Phys Rev Lett* 47(15):1060–1064.
6. Monchaux R, et al. (2007) Generation of a magnetic field by dynamo action in a turbulent flow of liquid sodium. *Phys Rev Lett* 98(4):044502.
7. Kulsrud RM, Zweibel EG (2008) On the origin of cosmic magnetic fields. *Rep Prog Phys* 71(4):046901.
8. Durrer D, Neronov A (2013) Cosmological magnetic fields: Their generation, evolution and observation. *Astron Astrophys Rev* 21:62.
9. Zweibel EG, Heiles C (1997) Magnetic fields in galaxies and beyond. *Nature* 385: 131–136.
10. Carilli CL, Taylor GB (2002) Cluster magnetic fields. *Annu Rev Astron Astrophys* 40: 319–348.
11. Vogt C, Enßlin TA (2005) A Bayesian view on Faraday rotation maps: Seeing the magnetic power spectra in galaxy clusters. *Astron Astrophys* 434(1):67–76.
12. Schekochihin AA, Cowley SC, Kulsrud RM, Hammett GW, Sharma P (2005) Plasma instabilities and magnetic field growth in clusters of galaxies. *Astrophys J* 629(1): 139–142.
13. Medvedev MV, Silva LO, Kamionkowski M (2006) Cluster magnetic fields from large-scale structure and galaxy cluster shocks. *Astrophys J* 642(1):L1–L4.
14. Ryu D, Kang H, Cho J, Das S (2008) Turbulence and magnetic fields in the large-scale structure of the universe. *Science* 320(5878):909–912.
15. Vazza F, Brüggen M, Gheller C, Wang P (2014) On the amplification of magnetic fields in cosmic filaments and galaxy clusters. *Mon Not R Astron Soc* 445(4):3706–3722.
16. Santos-Lima R, et al. (2014) Magnetic field amplification and evolution in turbulent collisionless magnetohydrodynamics: An application to the intracluster medium. *Astrophys J* 781(2):84.
17. Mogavero F, Schekochihin AA (2014) Models of magnetic field evolution and effective viscosity in weakly collisional extragalactic plasmas. *Mon Not R Astron Soc* 440(4): 3226–3242.
18. Miniati F, Beresnyak A (2015) Self-similar energetics in large clusters of galaxies. *Nature* 523(7558):59–62.
19. Forest CB, et al. (2015) The Wisconsin Plasma Astrophysics Laboratory. *J Plasma Phys* 81(5):345810501.
20. Meinecke J, et al. (2015) Developed turbulence and nonlinear amplification of magnetic fields in laboratory and astrophysical plasmas. *Proc Natl Acad Sci USA* 112(27):8211–8215.
21. Schekochihin AA, Cowley SC, Kulsrud RM, Rosin MS, Heinemann T (2008) Nonlinear growth of firehose and mirror fluctuations in astrophysical plasmas. *Phys Rev Lett* 100(8):081301.
22. Schoeffler K, Drake JF, Swisdak M (2011) The effects of plasma beta and anisotropy instabilities on the dynamics of reconnecting magnetic fields in the heliosheath. *Astrophys J* 743(1):70.
23. Kunz MW, Schekochihin AA, Stone JM (2014) Firehose and mirror instabilities in a collisionless shearing plasma. *Phys Rev Lett* 112(20):205003.
24. Riquelme MA, Quataert E, Verscharen D (2015) Particle-in-cell simulations of continuously driven mirror and ion cyclotron instabilities in high beta astrophysical and heliospheric plasmas. *Astrophys J* 800(1):27.
25. Sironi L, Narayan R (2015) Electron heating by the ion cyclotron instability in collisionless accretion flows. I. Compression-driven instabilities and the electron heating mechanism. *Astrophys J* 800(2):88.
26. Hellinger P, Trávníček PM (2015) Proton temperature-anisotropy-driven instabilities in weakly collisional plasmas: Hybrid simulations. *J Plasma Phys* 81(1):305810103.
27. Rincon F, Schekochihin AA, Cowley SC (2015) Non-linear mirror instability. *Mon Not R Astron Soc* 447(1):L45–L49.
28. Biermann L (1950) Über den ursprung der magnetfelder auf sternen und im interstellaren raum. *Z Naturforsch A* 5:65–71.
29. Weibel ES (1959) Spontaneously growing transverse waves in a plasma due to an anisotropic velocity distribution. *Phys Rev Lett* 2(3):83–84.
30. Schekochihin AA, Cowley SC, Taylor SF (2004) Simulations of the small-scale turbulent dynamo. *Astrophys J* 612(1):276–307.
31. Valentini F, Trávníček P, Califano F, Hellinger P, Mangeney A (2007) A hybrid-Vlasov model based on the current advance method for the simulation of collisionless magnetized plasma. *J Comput Phys* 225(1):753–770.
32. Alvelius K (1999) Random forcing of three-dimensional homogeneous turbulence. *Phys Fluids (1994)* 11(7):1880–1889.
33. Fried BD, Conte SD (1961) *The Plasma Dispersion Function* (Academic, New York).